JOURNAL OF THERMOPHYSICS AND HEAT TRANSFER
Vol. 20, No. 1, January–March 2006

Finite Volume Method for Radiation Heat Transfer in Graded Index Medium

L. H. Liu*
Harbin Institute of Technology, 150001 Harbin, People's Republic of China

Because a ray goes along a curved path determined by the Fermat principle, curved ray tracing is very difficult and complex in a graded index medium. To avoid the complicated and time-consuming computation of curved ray trajectories, a finite volume formulation is developed to solve the radiative-transfer problem in a multidimensional absorbing-emitting-scattering semitransparent graded index medium. Three test problems in radiative transfer are taken as examples to verify this finite volume formulation. The predicted temperature distributions and apparent directional emissivity are determined by the proposed method and compared with data in the references. The results show that the finite volume formulation presented in this paper has a good accuracy in solving the radiative transfer problem in a multidimensional absorbing-emitting-scattering semitransparent graded index medium.

Nomenclature

A	=	surface area of cell, m^2
b	=	asymmetry factor of scattering
D	=	direction cosine integrated over control solid angle
E_{rms}	=	rms error of apparent directional emissivity, defined in Eq. (27)
$\boldsymbol{e}_i$	=	unit outward normal vector at the ith surface of cell volume
H	=	height of medium, m
I	=	radiative intensity, W/m^3sr
I_b	=	blackbody radiative intensity, W/m^3sr
$\boldsymbol{i}, \boldsymbol{j}, \boldsymbol{k}$	=	unit vectors into the x, y, and z directions, respectively
L	=	thickness of slab, length, m
N_P	=	total number of surface for a cell
N_V	=	number of spatial control volumes
N_x, N_y, N_z	=	number of discretizations in x, y, and z directions, respectively
N_θ	=	number of polar angular discretizations
N_ξ	=	number of discretizations in ξ direction
N_φ	=	number of azimuthal angular discretizations
n	=	refractive index
n_i	=	refractive index at the ith surface
n_{P_i}	=	refractive index at node P_i
$\boldsymbol{r}$	=	spatial position vector
s	=	abscissa along the ray trajectory, m
$\boldsymbol{s}_1$	=	vector defined in Eq. (17b), $\boldsymbol{s}_1 = -\boldsymbol{i}\sin\varphi + \boldsymbol{j}\cos\varphi$
T	=	temperature, K
x, y, z	=	Cartesian coordinates in the coordinate system $x-o-y$
x', y'	=	Cartesian coordinates in the coordinate system $x'-o-y'$
α, β, γ	=	refractive index derivatives, defined in Eq. (9)
ΔV	=	volume of control volume, m^3
$\Delta\theta$	=	polar angle step, rad
$\Delta\varphi$	=	azimuthal angle step, rad
$\Delta\Omega$	=	control solid angle, sr
ε	=	emissivity
$\varepsilon_{\varphi_{\text{out}}}$	=	apparent directional emissivity
$\varepsilon_{\varphi_{\text{out}},\text{FVM}}$	=	apparent directional emissivity obtained by finite volume method
$\varepsilon_{\varphi_{\text{out}},\text{ray-tracing}}$	=	apparent directional emissivity obtained by ray-tracing method
η	=	direction cosine, $\eta = \sin\theta\sin\varphi$
θ	=	polar angle, rad
κ_a	=	absorption coefficient, m^{-1}
κ_s	=	scattering coefficient, m^{-1}
μ	=	direction cosine, $= \sin\theta\cos\varphi$
ξ	=	direction cosine, $= \cos\theta$
σ	=	Stefan–Boltzmann constant, W/m^2K^4
$\tau_{H/2}$	=	optical thickness based on half height, $\tau_{H/2} = (\kappa_a + \kappa_s)H/2$
τ_L	=	optical thickness of slab, $\tau_L = (\kappa_a + \kappa_s)L$
Φ	=	scattering phase function
$\bar{\Phi}$	=	averaged scattering phase function defined in Eq. (20g)
φ	=	azimuthal angle, rad
φ_{out}	=	emerging angle, rad
φ_0	=	transformation angle of coordinate system, rad
χ_θ, χ_φ	=	coefficients of the discretization equation, defined in Eqs. (20b) and (20c)
Ω	=	solid angle, sr
$\boldsymbol{\Omega}$	=	vector of radiation direction, $\boldsymbol{\Omega} = \boldsymbol{i}\mu + \boldsymbol{j}\eta + \boldsymbol{k}\xi$
ω	=	single scattering albedo, $= \kappa_s/(\kappa_a + \kappa_s)$
∇	=	spatial divergence operator, $= \boldsymbol{i}(\partial/\partial x) + \boldsymbol{j}(\partial/\partial y) + \boldsymbol{k}(\partial/\partial z)$

Subscripts

i	=	value at the ith surface of cell
L	=	at position $z = L$
P	=	value at the center of cell volume
P_i	=	value at the center of cell volume neighboring pth cell
0	=	at position $z = 0$

Superscripts

m, n, m', n', $m \pm 1/2$, $n \pm 1/2$	=	angular direction of radiation

I. Introduction

BECAUSE of the structural characteristics of a material or a possible temperature dependency, the refractive index of a medium can be a function of spatial position. In this case, rays propagating

Received 26 July 2004; revision received 21 February 2005; accepted for publication 27 February 2005.

*Professor, School of Energy Science and Engineering, 92 West Dazhi Street; lhliu@hit.edu.cn.

inside the medium are not straight lines, but curved lines determined by the Fermat principle.[1] Radiative heat transfer in a semitransparent medium with variable spatial refractive index (graded index) is of great interest in thermo-optical systems and has evoked the wide interest of many researchers. As early as 1993, Siegel and Spuckler[2] analyzed variable refractive index effects on radiation in semitransparent scattering multilayered regions and pointed out that refractive indices of semitransparent sublayers inside a composite could have considerable effect on the temperature distribution and radiative flux fields. Curved ray tracing is the main difficulty for the solution of radiative transfer in a medium with variable spatial refractive index. Recently, many ray-tracing techniques have been presented to solve the radiative-transfer problem in a semitransparent medium with graded refractive index. Ben Abdallah and coworkers[3–6] developed and used a curved ray-tracing technique to analyze radiative heat transfer in an absorbing-emitting semitransparent medium with variable spatial refractive index. Liu[7] presented a discrete curved ray-tracing method, in which the curved ray trajectory is locally treated as straight line. Based on the discrete curved ray-tracing technique, Liu et al.[8] developed a Monte Carlo discrete curved ray-tracing method, in which the Monte Carlo method is combined with the discrete curved ray-tracing method. Ben Abdallah et al.[9] proposed an integrated form of the radiative-transfer equation along the curved ray trajectory inside refracting cylindrical media. Huang et al.[10,11] presented a combined curved ray-tracing and pseudosource adding method for radiative heat transfer in a one-dimensional semitransparent medium with graded refractive index. Because the ray goes along a curved path determined by the Fermat principle, curved ray tracing is very difficult and complex in a medium with variable spatial refractive index. Therefore, methods based on curved ray-tracing techniques are mainly limited to one-dimensional radiative-transfer problems. The multidimensional radiative-transfer problem within a graded index medium has been addressed only by Ben Abdallah and Le Dez[4] for the apparent emissivity of a two-dimensional rectangular medium with spatially varying refractive index. A general method applicable to radiative transfer inside multidimensional semitransparent media with a graded refractive index is not presently available.

The finite volume method (FVM), because of its general applicability and its ability to treat complex geometry, is today probably the most popular method to solve the radiative-transfer problem in a medium with uniform refractive index. The first finite volume formulations of the radiative-transfer equation were given by Raithby and coworkers.[12–14] Different schemes have been proposed by Chai and coworkers.[15–17] However, because the ray goes along a curved path, the streaming operator d/ds in the radiative-transfer equation contains not only the spatial differentiating operators but also the angular operators; therefore, the divergence theorem and then the FVM cannot be directly used to solve the radiative-transfer problem within a medium having a graded refractive index. To avoid the complicated and time-consuming computation of a curved ray trajectory and to develop a general method applicable to radiative transfer inside multidimensional semitransparent media with graded refractive index, in this paper we first transform the radiative-transfer equation. After that, based on the transformed equation, we develop a finite volume formulation for radiative heat transfer in a multidimensional semitransparent medium with graded refractive index. Finally, some radiative-transfer problems inside a semitransparent graded index medium are taken as examples to verify this finite volume formulation.

II. Mathematical Formulation

A. Radiative-Transfer Equation

The radiative-transfer equation at steady state in an absorbing-emitting-scattering semitransparent graded index medium is given by

$$n^2 \frac{\mathrm{d}}{\mathrm{d}s}\left[\frac{I(\boldsymbol{r},\Omega)}{n^2}\right] + (\kappa_a+\kappa_s) I(\boldsymbol{r},\Omega) = n^2\kappa_a I_b(\boldsymbol{r}) + \frac{\kappa_s}{4\pi}\int_{4\pi} I(\boldsymbol{r},\Omega')\Phi(\Omega',\Omega)\,\mathrm{d}\Omega' \tag{1}$$

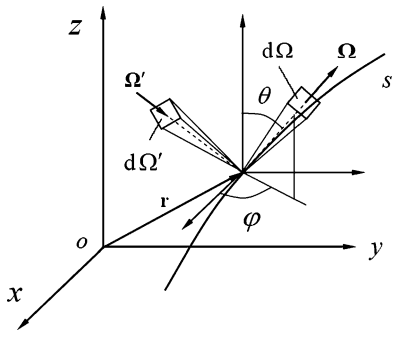

Fig. 1 Cartesian coordinate system.

To use the finite volume method, Eq. (1) needs to be transformed so that the divergence theorem can be applied to integrate the radiative-transfer equation. In the Cartesian coordinate system shown in Fig. 1, the radiative intensity is a function of variables x, y, z, θ, and φ. When moving along one given path, the streaming operator d/ds can be split into

$$\frac{\mathrm{d}}{\mathrm{d}s} = \frac{\mathrm{d}x}{\mathrm{d}s}\frac{\partial}{\partial x} + \frac{\mathrm{d}y}{\mathrm{d}s}\frac{\partial}{\partial y} + \frac{\mathrm{d}z}{\mathrm{d}s}\frac{\partial}{\partial z} + \frac{\mathrm{d}\theta}{\mathrm{d}s}\frac{\partial}{\partial \theta} + \frac{\mathrm{d}\varphi}{\mathrm{d}s}\frac{\partial}{\partial \varphi} \tag{2}$$

Because $\mathrm{d}x = \mu\,\mathrm{d}s$, $\mathrm{d}y = \eta\,\mathrm{d}s$, and $\mathrm{d}z = \xi\,\mathrm{d}s$, we have

$$\frac{\mathrm{d}}{\mathrm{d}s} = \mu\frac{\partial}{\partial x} + \eta\frac{\partial}{\partial y} + \xi\frac{\partial}{\partial z} + \frac{\mathrm{d}\theta}{\mathrm{d}s}\frac{\partial}{\partial \theta} + \frac{\mathrm{d}\varphi}{\mathrm{d}s}\frac{\partial}{\partial \varphi} \tag{3}$$

where μ, η, and ξ are the direction cosines of the local tangent vector of ray trajectory along the Cartesian coordinate x, y, and z directions, and given by

$$\mu = \sin\theta\cos\varphi \tag{4a}$$

$$\eta = \sin\theta\sin\varphi \tag{4b}$$

$$\xi = \cos\theta \tag{4c}$$

By differentiating Eq. (4) with respect to s, we have

$$\frac{\mathrm{d}\mu}{\mathrm{d}s} = \frac{\mathrm{d}(\sin\theta\cos\varphi)}{\mathrm{d}s} = \cos\theta\cos\varphi\frac{\mathrm{d}\theta}{\mathrm{d}s} - \sin\theta\sin\varphi\frac{\mathrm{d}\varphi}{\mathrm{d}s} \tag{5a}$$

$$\frac{\mathrm{d}\eta}{\mathrm{d}s} = \frac{\mathrm{d}(\sin\theta\sin\varphi)}{\mathrm{d}s} = \cos\theta\sin\varphi\frac{\mathrm{d}\theta}{\mathrm{d}s} + \sin\theta\cos\varphi\frac{\mathrm{d}\varphi}{\mathrm{d}s} \tag{5b}$$

$$\frac{\mathrm{d}\xi}{\mathrm{d}s} = -\sin\theta\frac{\mathrm{d}\theta}{\mathrm{d}s} \tag{5c}$$

The result is

$$\frac{\mathrm{d}\varphi}{\mathrm{d}s} = \frac{1}{\sin\theta}\left(\cos\varphi\frac{\mathrm{d}\eta}{\mathrm{d}s} - \sin\varphi\frac{\mathrm{d}\mu}{\mathrm{d}s}\right) \tag{6a}$$

$$\frac{\mathrm{d}\theta}{\mathrm{d}s} = -\frac{1}{\sin\theta}\frac{\mathrm{d}\xi}{\mathrm{d}s} \tag{6b}$$

From the ray equations[1]

$$\frac{\mathrm{d}}{\mathrm{d}s}(n\mu) = \frac{\partial n}{\partial x} \tag{7a}$$

$$\frac{\mathrm{d}}{\mathrm{d}s}(n\eta) = \frac{\partial n}{\partial y} \tag{7b}$$

$$\frac{\mathrm{d}}{\mathrm{d}s}(n\xi) = \frac{\partial n}{\partial z} \tag{7c}$$

we have

$$\frac{\mathrm{d}\mu}{\mathrm{d}s} = \frac{1}{n}\left[\frac{\partial n}{\partial x} - \mu\left(\mu\frac{\partial n}{\partial x} + \eta\frac{\partial n}{\partial y} + \xi\frac{\partial n}{\partial z}\right)\right]$$
$$= \alpha - \mu(\mu\alpha + \eta\beta + \xi\gamma) \tag{8a}$$

$$\frac{\mathrm{d}\eta}{\mathrm{d}s} = \frac{1}{n}\left[\frac{\partial n}{\partial y} - \eta\left(\mu\frac{\partial n}{\partial x} + \eta\frac{\partial n}{\partial y} + \xi\frac{\partial n}{\partial z}\right)\right]$$
$$= \beta - \eta(\mu\alpha + \eta\beta + \xi\gamma) \tag{8b}$$

$$\frac{\mathrm{d}\xi}{\mathrm{d}s} = \frac{1}{n}\left[\frac{\partial n}{\partial z} - \xi\left(\mu\frac{\partial n}{\partial x} + \eta\frac{\partial n}{\partial y} + \xi\frac{\partial n}{\partial z}\right)\right]$$
$$= \gamma - \xi(\mu\alpha + \eta\beta + \xi\gamma) \tag{8c}$$

where the refractive index derivatives α, β, and γ are defined respectively as

$$\alpha = \frac{1}{n}\frac{\partial n}{\partial x} = \frac{1}{2n^2}\frac{\partial n^2}{\partial x} \tag{9a}$$

$$\beta = \frac{1}{n}\frac{\partial n}{\partial y} = \frac{1}{2n^2}\frac{\partial n^2}{\partial y} \tag{9b}$$

$$\gamma = \frac{1}{n}\frac{\partial n}{\partial z} = \frac{1}{2n^2}\frac{\partial n^2}{\partial z} \tag{9c}$$

Substituting Eq. (8) into Eq. (6) results in the following relations:

$$\frac{\mathrm{d}\varphi}{\mathrm{d}s} = \frac{1}{\sin\theta}[\beta\cos\varphi - \alpha\sin\varphi] \tag{10a}$$

$$\frac{\mathrm{d}\theta}{\mathrm{d}s} = \frac{1}{\sin\theta}[\xi(\mu\alpha + \eta\beta + \xi\gamma) - \gamma] \tag{10b}$$

Therefore, the streaming operator d/ds in Eq. (3) can be written as

$$\frac{\mathrm{d}}{\mathrm{d}s} = \mu\frac{\partial}{\partial x} + \eta\frac{\partial}{\partial y} + \xi\frac{\partial}{\partial z} + \frac{1}{\sin\theta}\left\{[\xi(\mu\alpha + \eta\beta + \xi\gamma) - \gamma]\frac{\partial}{\partial\theta} + [\beta\cos\varphi - \alpha\sin\varphi]\frac{\partial}{\partial\varphi}\right\} \tag{11}$$

By using the following relations,

$$n^2\mu\frac{\partial}{\partial x}\left(\frac{I}{n^2}\right) = \mu\frac{\partial I}{\partial x} - \frac{2\mu I}{n}\frac{\partial n}{\partial x} = \mu\frac{\partial I}{\partial x} - 2\alpha\mu I \tag{12a}$$

$$n^2\eta\frac{\partial}{\partial y}\left(\frac{I}{n^2}\right) = \eta\frac{\partial I}{\partial y} - \frac{2\eta I}{n}\frac{\partial n}{\partial y} = \eta\frac{\partial I}{\partial y} - 2\beta\eta I \tag{12b}$$

$$n^2\xi\frac{\partial}{\partial z}\left(\frac{I}{n^2}\right) = \xi\frac{\partial I}{\partial z} - \frac{2\xi I}{n}\frac{\partial n}{\partial \xi} = \xi\frac{\partial I}{\partial z} - 2\gamma\xi I \tag{12c}$$

$$n^2\frac{\partial}{\partial\theta}\left(\frac{I}{n^2}\right) = \frac{\partial I}{\partial\theta} \tag{12d}$$

$$n^2\frac{\partial}{\partial\varphi}\left(\frac{I}{n^2}\right) = \frac{\partial I}{\partial\varphi} \tag{12e}$$

The radiative-transfer equation can be expressed in a nonconservative form as

$$\mu\frac{\partial I(\boldsymbol{r},\Omega)}{\partial x} + \eta\frac{\partial I(\boldsymbol{r},\Omega)}{\partial y} + \xi\frac{\partial I(\boldsymbol{r},\Omega)}{\partial z} + \frac{1}{\sin\theta}\left\{[\xi(\mu\alpha + \eta\beta + \xi\gamma) - \gamma]\frac{\partial I(\boldsymbol{r},\Omega)}{\partial\theta} + [\beta\cos\varphi - \alpha\sin\varphi]\frac{\partial I(\boldsymbol{r},\Omega)}{\partial\varphi}\right\} + [\kappa_a + \kappa_s - 2(\mu\alpha + \eta\beta + \xi\gamma)]I(\boldsymbol{r},\Omega) = n^2\kappa_a I_b + \frac{\kappa_s}{4\pi}\int_{4\pi} I(\boldsymbol{r},\Omega')\Phi(\Omega,\Omega')\,\mathrm{d}\Omega' \tag{13}$$

From Eq. (13), by using the following relationships,

$$(\beta\cos\varphi - \alpha\sin\varphi)\frac{\partial I(\boldsymbol{r},\Omega)}{\partial\varphi} = \frac{\partial}{\partial\varphi}[(\beta\cos\varphi - \alpha\sin\varphi)I(\boldsymbol{r},\Omega)] + [\beta\sin\varphi + \alpha\cos\varphi]I(\boldsymbol{r},\Omega) \tag{14a}$$

$$[\xi(\mu\alpha + \eta\beta + \xi\gamma) - \gamma]\frac{\partial I(\boldsymbol{r},\Omega)}{\partial\theta} = \frac{\partial}{\partial\theta}\{[\xi(\mu\alpha + \eta\beta + \xi\gamma) - \gamma] \times I(\boldsymbol{r},\Omega)\} - (\alpha\cos\varphi + \beta\sin\varphi)I(\boldsymbol{r},\Omega) + 2\sin\theta(\mu\alpha + \eta\beta + \xi\gamma)I(\boldsymbol{r},\Omega) \tag{14b}$$

the conservative form of radiative-transfer equation can be written as

$$\mu\frac{\partial I(\boldsymbol{r},\Omega)}{\partial x} + \eta\frac{\partial I(\boldsymbol{r},\Omega)}{\partial y} + \xi\frac{\partial I(\boldsymbol{r},\Omega)}{\partial z} + \frac{1}{\sin\theta}\frac{\partial}{\partial\theta}\{[\xi(\mu\alpha + \eta\beta + \xi\gamma) - \gamma]I(\boldsymbol{r},\Omega)\} + \frac{1}{\sin\theta}\frac{\partial}{\partial\varphi}\{[\beta\cos\varphi - \alpha\sin\varphi]I(\boldsymbol{r},\Omega)\} + (\kappa_a + \kappa_s)I(\boldsymbol{r},\Omega) = n^2\kappa_a I_b + \frac{\kappa_s}{4\pi}\int_{4\pi} I(\boldsymbol{r},\Omega')\Phi(\Omega,\Omega')\,\mathrm{d}\Omega' \tag{15}$$

or expressed in divergence form as

$$\boldsymbol{\Omega}\cdot\nabla I(\boldsymbol{r},\Omega) + \frac{1}{2n^2\sin\theta}\frac{\partial}{\partial\theta}\{[I(\boldsymbol{r},\Omega)(\xi\boldsymbol{\Omega} - \boldsymbol{k})\cdot\nabla n^2]\} + \frac{1}{2n^2\sin\theta}\frac{\partial}{\partial\varphi}\left\{I(\boldsymbol{r},\Omega)\left[\boldsymbol{s}_1\cdot\nabla n^2\right]\right\} + (\kappa_a + \kappa_s)I(\boldsymbol{r},\Omega) = n^2\kappa_a I_b + \frac{\kappa_s}{4\pi}\int_{4\pi} I(\boldsymbol{r},\Omega')\Phi(\Omega,\Omega')\,\mathrm{d}\Omega' \tag{16}$$

where

$$\boldsymbol{\Omega} = \boldsymbol{i}\mu + \boldsymbol{j}\eta + \boldsymbol{k}\xi = \boldsymbol{i}\sin\theta\cos\varphi + \boldsymbol{j}\sin\theta\sin\varphi + \boldsymbol{k}\cos\theta \tag{17a}$$

$$\boldsymbol{s}_1 = -\boldsymbol{i}\sin\varphi + \boldsymbol{j}\cos\varphi \tag{17b}$$

Terms involving a partial derivative with respect to an angular coordinate in Eqs. (15) or (16) are referred as angular redistribution terms, which account for the curvature of the optical path in the graded index medium.

B. Discretization

Equation (16) involves not only spatial differentiation but also angular integration. To solve this equation numerically, both the spatial domain and the angular domain must be discretized. Similar to the treatment of the finite volume method for radiative heat transfer in a medium with uniform refractive index, the spatial computational domain is subdivided into N_V spatial control volumes. The types of control volumes can vary from triangular to quadrilateral for two-dimensional problems and from tetrahedral, prismatic, pyramidal, to hexahedral for three-dimensional problems. Considering that Eq. (16) contains two angular redistribution terms, we employ the piecewise constant angular quadrature. The total solid angle is subdivided into $N_\theta \times N_\varphi$ control solid angles with polar and azimuthal steps, $\Delta\theta = \theta^{m+1/2} - \theta^{m-1/2}$ and $\Delta\varphi = \varphi^{n+1/2} - \varphi^{n-1/2}$, respectively. Integrating Eq. (16) over cell volume and solid angle along a discrete direction $\Omega^{m,n}$ with the assumption that the magnitude of intensity in a given direction is constant within control cell volume and control solid angle, and using the divergence theorem leads to

the following discretized equation:

$$\sum_{i=1}^{N_P} I_i^{m,n} A_i \int_{\Delta\Omega^{m,n}} (\boldsymbol{\Omega}\cdot\boldsymbol{e}_i)\,\mathrm{d}\Omega + \frac{1}{2n_P^2}\left\{ I_P^{m+\frac{1}{2},n} \sum_{i=1}^{N_P}\left[\left(\int_{\varphi^{n-\frac{1}{2}}}^{\varphi^{n+\frac{1}{2}}} [\xi\boldsymbol{\Omega}-\boldsymbol{k}]^{m+\frac{1}{2}}\,\mathrm{d}\varphi\right)\cdot\boldsymbol{e}_i\right] A_i n_i^2 - I_P^{m-\frac{1}{2},n}\sum_{i=1}^{N_P}\left[\left(\int_{\varphi^{n-\frac{1}{2}}}^{\varphi^{n+\frac{1}{2}}} [\xi\boldsymbol{\Omega}-\boldsymbol{k}]^{m-\frac{1}{2}}\,\mathrm{d}\varphi\right)\cdot\boldsymbol{e}_i\right] A_i n_i^2\right\} + \frac{\Delta\theta}{2n_P^2}\left\{ I_P^{m,n+\frac{1}{2}}\sum_{i=1}^{N_P}\left(\boldsymbol{s}_1^{n+\frac{1}{2}}\cdot\boldsymbol{e}_i\right) A_i n_i^2 - I_P^{m,n-\frac{1}{2}}\sum_{i=1}^{N_P}\left(\boldsymbol{s}_1^{n-\frac{1}{2}}\cdot\boldsymbol{e}_i\right) A_i n_i^2\right\} + \Delta V_P \Delta\Omega^{m,n}(\kappa_{a,P}+\kappa_{s,P}) I_P^{m,n} = \Delta V_P \Delta\Omega^{m,n} n_P^2 \kappa_{a,P} I_{b,P} + \Delta V_P \Delta\Omega^{m,n}\frac{\kappa_{s,P}}{4\pi}\sum_{m',n'} I_P^{m',n'}\Phi_P^{m',n';m,n}\Delta\Omega^{m',n'} \tag{18}$$

Equation (18) can be compactly rewritten as

$$\sum_{i=1}^{N_P} A_i D_i^{m,n} I_i^{m,n} + \chi_\theta^{m+\frac{1}{2},n} I_P^{m+\frac{1}{2},n} - \chi_\theta^{m-\frac{1}{2},n} I_P^{m-\frac{1}{2},n} + \chi_\varphi^{m,n+\frac{1}{2}} I_P^{m,n+\frac{1}{2}} - \chi_\varphi^{m,n-\frac{1}{2}} I_P^{m,n-\frac{1}{2}} + \Delta V_P \Delta\Omega^{m,n}(\kappa_{a,P}+\kappa_{s,P}) I_P^{m,n} = \Delta V_P \Delta\Omega^{m,n} n_P^2 \kappa_{a,P} I_{b,P} + \Delta V_P \Delta\Omega^{m,n}\frac{\kappa_{s,P}}{4\pi}\sum_{m',n'} I_P^{m',n'}\bar{\Phi}_P^{m',n';m,n}\Delta\Omega^{m',n'} \tag{19}$$

where

$$D_i^{m,n} = \int_{\Delta\Omega^{m,n}} (\boldsymbol{\Omega}\cdot\boldsymbol{e}_i)\,\mathrm{d}\Omega \tag{20a}$$

$$\chi_\theta^{m+\frac{1}{2},n} = \frac{1}{2n_P^2}\sum_{i=1}^{N_P}\left[\left(\int_{\varphi^{n-\frac{1}{2}}}^{\varphi^{n+\frac{1}{2}}} [\xi\boldsymbol{\Omega}-\boldsymbol{k}]^{m+\frac{1}{2}}\,\mathrm{d}\varphi\right)\cdot\boldsymbol{e}_i\right] A_i n_i^2 \tag{20b}$$

$$\chi_\theta^{m-\frac{1}{2},n} = \frac{1}{2n_P^2}\sum_{i=1}^{N_P}\left[\left(\int_{\varphi^{n-\frac{1}{2}}}^{\varphi^{n+\frac{1}{2}}} [\xi\boldsymbol{\Omega}-\boldsymbol{k}]^{m-\frac{1}{2}}\,\mathrm{d}\varphi\right)\cdot\boldsymbol{e}_i\right] A_i n_i^2 \tag{20c}$$

$$\chi_\varphi^{m,n+\frac{1}{2}} = \frac{\Delta\theta}{2n_P^2}\sum_{i=1}^{N_P}\left(\boldsymbol{s}_1^{n+\frac{1}{2}}\cdot\boldsymbol{e}_i\right) A_i n_i^2 \tag{20d}$$

$$\chi_\varphi^{m,n-\frac{1}{2}} = \frac{\Delta\theta}{2n_P^2}\sum_{i=1}^{N_P}\left(\boldsymbol{s}_1^{n-\frac{1}{2}}\cdot\boldsymbol{e}_i\right) A_i n_i^2 \tag{20e}$$

$$\Delta\Omega^{m,n} = \int_{\varphi^{n-\frac{1}{2}}}^{\varphi^{n+\frac{1}{2}}}\int_{\theta^{m-\frac{1}{2}}}^{\theta^{m+\frac{1}{2}}} \sin\theta\,\mathrm{d}\theta\,\mathrm{d}\varphi \tag{20f}$$

$$\bar{\Phi}_P^{m',n';m,n} = \frac{1}{\Delta\Omega^{m',n'}\Delta\Omega^{m,n}}\int_{\Delta\Omega^{m,n}}\int_{\Delta\Omega^{m',n'}} \Phi(\Omega',\Omega)\,\mathrm{d}\Omega'\,\mathrm{d}\Omega \tag{20g}$$

To close Eq. (19), relations are needed between the intensities on the cell surfaces and the cell center intensities. One appropriate closure relation is based on the step schemes that set the downstream surface intensities equal to the upstream center intensities. Those are

$$A_i D_i^{m,n} I_i^{m,n} = \left(n_i^2/n_P^2\right)\max\left(A_i D_i^{m,n},0\right) I_P^{m,n} - \left(n_i^2/n_{P_i}^2\right)\max\left(-A_i D_i^{m,n},0\right) I_{P_i}^{m,n} \tag{21a}$$

$$\chi_\theta^{m+\frac{1}{2},n} I_P^{m+\frac{1}{2},n} = \max\left(\chi_\theta^{m+\frac{1}{2},n},0\right) I_P^{m,n} - \max\left(-\chi_\theta^{m+\frac{1}{2},n},0\right) I_P^{m+1,n} \tag{21b}$$

$$\chi_\theta^{m-\frac{1}{2},n} I_P^{m-\frac{1}{2},n} = \max\left(\chi_\theta^{m-\frac{1}{2},n},0\right) I_P^{m-1,n} - \max\left(-\chi_\theta^{m-\frac{1}{2},n},0\right) I_P^{m,n} \tag{21c}$$

$$\chi_\varphi^{m,n+\frac{1}{2}} I_P^{m,n+\frac{1}{2}} = \max\left(\chi_\varphi^{m,n+\frac{1}{2}},0\right) I_P^{m,n} - \max\left(-\chi_\varphi^{m,n+\frac{1}{2}},0\right) I_P^{m,n+1} \tag{21d}$$

$$\chi_\varphi^{m,n-\frac{1}{2}} I_P^{m,n-\frac{1}{2}} = \max\left(\chi_\varphi^{m,n-\frac{1}{2}},0\right) I_P^{m,n-1} - \max\left(-\chi_\varphi^{m,n-\frac{1}{2}},0\right) I_P^{m,n} \tag{21e}$$

where P_i is the neighboring cell of cell P with the ith surface as the common face between P and P_i, and $I_{P_i}^{m,n}$ denotes the intensity within cell P_i. In Eq. (21a), the factors n_i^2/n_P^2 and $n_i^2/n_{P_i}^2$ account for the change of solid angle when a radiative energy bundle passes into a medium with different refractive index. By moving the forward scattering term from the right side of Eq. (19) to the left side and using the closure relations given in Eq. (21), the final discretized equation of radiative transfer in a three-dimensional medium with variable spatial refractive index becomes

$$\left[\sum_{i=1}^{N_P}\frac{n_i^2}{n_P^2}\max\left(A_i D_i^{m,n},0\right) + \max\left(\chi_\theta^{m+\frac{1}{2},n},0\right) + \max\left(-\chi_\theta^{m-\frac{1}{2},n},0\right) + \max\left(\chi_\varphi^{m,n+\frac{1}{2}},0\right) + \max\left(-\chi_\varphi^{m,n-\frac{1}{2}},0\right) + \Delta V_P\Delta\Omega^{m,n}(\kappa_{a,P}+\kappa_{s,P}) - \Delta V_P\Delta\Omega^{m,n}\frac{\kappa_{s,P}}{4\pi}\bar{\Phi}_P^{m,n;m,n}\Delta\Omega^{m,n}\right] I_P^{m,n} = \sum_{i=1}^{N_P}\frac{n_i^2}{n_{P_i}^2}\max\left(-A_i D_i^{m,n},0\right) I_{P_i}^{m,n} + \max\left(-\chi_\theta^{m+\frac{1}{2},n},0\right) I_P^{m+1,n} + \max\left(\chi_\theta^{m-\frac{1}{2},n},0\right) I_P^{m-1,n} + \max\left(-\chi_\varphi^{m,n+\frac{1}{2}},0\right) I_P^{m,n+1} + \max\left(\chi_\varphi^{m,n-\frac{1}{2}},0\right) I_P^{m,n-1} + \Delta V_P\Delta\Omega^{m,n} n_P^2\kappa_{a,P} I_{b,P} + \Delta V_P\Delta\Omega^{m,n}\frac{\kappa_{s,P}}{4\pi} \times \sum_{m',n';m\neq m',n\neq n'} I_P^{m',n'}\bar{\Phi}_P^{m',n';m,n}\Delta\Omega^{m',n'} \tag{22}$$

Equation (22) is a general finite volume formulation for the radiative transfer inside multidimensional semitransparent media with graded refractive index. It is applicable for any type of volume cell shape, structured or unstructured.

The preceding discretization is carried out in one discrete ordinate direction. The same discretization procedure is applied to all discrete ordinate directions. This forms a set of algebraic equations. The solution procedure and the iteration method applied to the discretized equation for a medium with variable spatial refractive index are similar to those for the medium with uniform refractive index. The details can be seen in Refs. 12–18 and will not be repeated here.

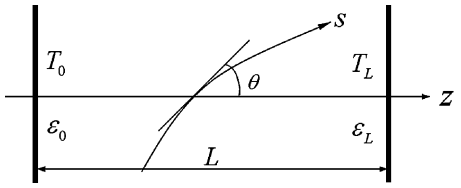

Fig. 2 Physical geometry of slab.

III. Results and Discussion

Based on the theoretical and numerical analyses just carried out, a computer code that is capable of modeling multidimensional radiative-transfer problems in a graded index medium has been developed. Grid-refinement studies were also performed for the physical model to ensure that the essential physics are independent of grid size. To help validate the finite volume formulation just presented, three test problems are examined. The test cases are selected because exact, or at lease very precise, solutions of the radiative-transfer equation exist for comparison with the finite volume solution. For the following numerical study, the maximum iteration relative error 10^{-4} of desired variable is taken as the stopping criterion for the iteration. To check the computational accuracy of FVM, the maximum relative error based on data in the references is defined as

maximum relative error

$$= \max \left| \frac{\text{data obtained by FVM-data in references}}{\text{data in references}} \right| \tag{23}$$

A. Radiative Equilibrium in a One-Dimensional Slab

As shown in Fig. 2, we consider a problem of radiative equilibrium in a one-dimensional semitransparent gray absorbing-emitting-scattering slab with thickness L. The boundaries are opaque, diffuse, and gray walls. The emissivities of the bounding walls are ε_0 and ε_L, and the temperatures of the bounding walls are $T_0 = 1000$ K and $T_L = 1500$ K, respectively. The scattering phase function is assumed to be linear as $\Phi(\Omega', \Omega) = 1 + b(\Omega \cdot \Omega')$. The absorption coefficient κ_a and scattering coefficient κ_s are uniform over the slab, but the refractive index n of the medium varies with coordinate z. The boundary conditions are given by

$$I(0, \xi) = \varepsilon_0 n_0^2 \frac{\sigma T_0^4}{\pi} + 2(1-\varepsilon_0) \int_{-1}^{0} I(0, \xi') \xi' \, \mathrm{d}\xi' \qquad \xi \geq 0 \tag{24a}$$

$$I(L, \xi) = \varepsilon_L n_L^2 \frac{\sigma T_L^4}{\pi} + 2(1-\varepsilon_L) \int_{0}^{1} I(L, \xi') \xi' \, \mathrm{d}\xi' \qquad \xi \leq 0 \tag{24b}$$

The FVM is applied to this one-dimensional problem. Linearly and sinusoidally varying refractive indices are considered. The regions of $z \in [0, L]$ and $\xi = \cos\theta \in [-1, 1]$ are uniformly divided into $N_z = 500$ and $N_\xi = 500$ parts, respectively. At radiative equilibrium, the temperature distribution within the medium is determined by

$$T(z) = \left[\frac{\pi}{2\sigma n^2(z)} \sum_{m=1}^{N_\xi} I(z, \xi^m) \Delta\xi \right]^{0.25} \tag{25}$$

The temperature distribution within the slab is shown in Fig. 3 for two values of optical thickness, namely, $\tau_L = 1.0$ and 3.0, in the case of $n(z) = 1.2 + 0.6z/L$, $\varepsilon_0 = \varepsilon_L = 1$, and $\omega = 0$. This case was also used as a test case by Huang et al.[11] using the pseudo source adding method. As shown in Fig. 3, the FVM results are in good agreement with the results obtained by using the pseudo source adding method. The maximum relative error based on the data in Ref. 11 is less than 1%. The effects of number of control volumes and angular discretization are shown in Fig. 4 for the case of $n(z) = 1.2 + 0.6z/L$, $\tau_L = 1$, $\varepsilon_0 = \varepsilon_L = 1$, and $\omega = 0$. The comparison is quite good, even with a mesh of only $N_z \times N_\xi = 10 \times 10$.

An anisotropically scattering slab with single scattering albedo $\omega = 0.8$ is studied by using FVM. The slab is bounded by black walls, and the slab optical thickness is $\tau_L = 1.0$. The refractive index of medium within the slab varies linearly with axis coordinate as $n(z) = 1.2 + 0.6z/L$. Liu et al.[19] studied this case using the Monte Carlo curved ray-tracing method. The temperature distributions within the slab are shown in Fig. 5 for two different values of asymmetry factor, namely, $b = 1$ and -1, and compared to the results obtained from the Monte Carlo curved ray-tracing method. The FVM results agree with those of the Monte Carlo curved ray-tracing method very well. The maximum relative error based on the data in Ref. 19 is less than 3%.

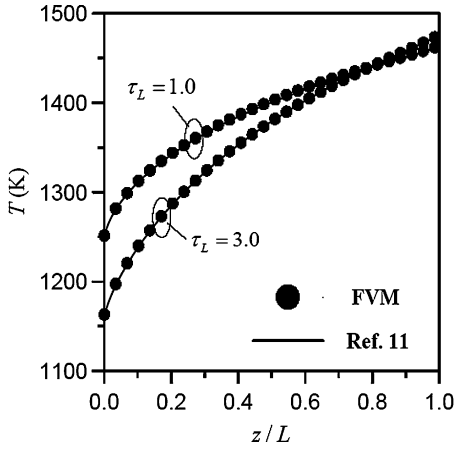

Fig. 3 Temperature distribution within a slab for the case of $n(z) = 1.2 + 0.6z/L$, $\varepsilon_0 = \varepsilon_L = 1$, and $\omega = 0$.

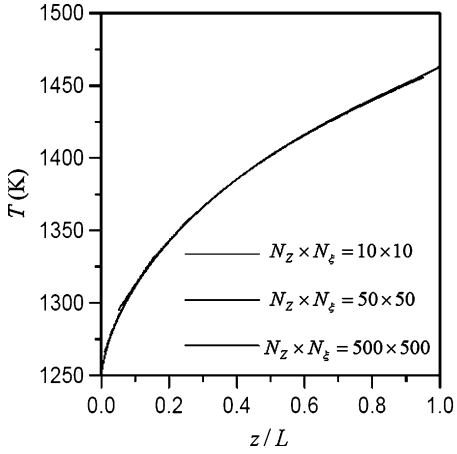

Fig. 4 Effects of number of control volumes and angular discretization in the case of $n(z) = 1.2 + 0.6z/L$, $\tau_L = 1$, $\varepsilon_0 = \varepsilon_L = 1$, and $\omega = 0$.

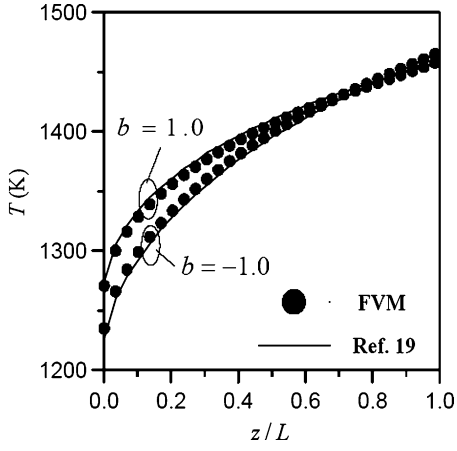

Fig. 5 Temperature distribution within a slab for the case of $n(z) = 1.2 + 0.6z/L$, $\tau_L = 1$, $\varepsilon_0 = \varepsilon_L = 1$, and $\omega = 0.8$.

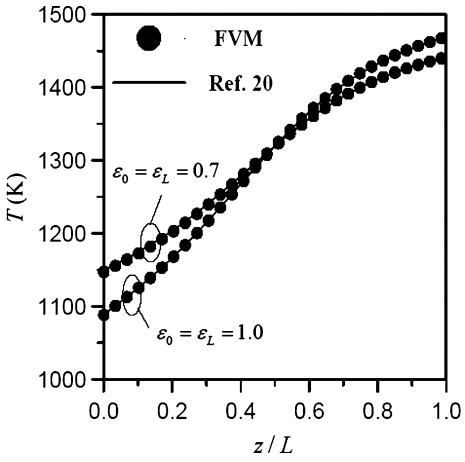

Fig. 6 Temperature distribution within a slab for the case of $n(z) = 1.8 - 0.6\sin(\pi z/L)$, $\tau_L = 1$, and $\omega = 0$.

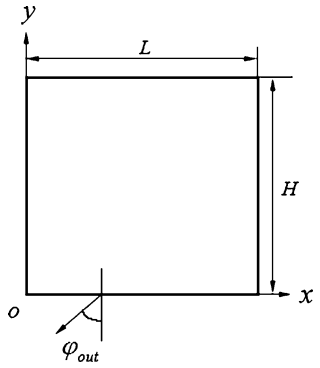

Fig. 7 Two-dimensional rectangular medium and the coordinate system.

A nonlinear refractive index is also studied by using FVM. The refractive index of the medium varies sinusoidally with axis coordinate as $n(z) = 1.8 - 0.6\sin(\pi z/L)$. The medium is nonscattering, and the slab optical thickness is $\tau_L = 1.0$. Figure 6 shows the temperature distributions within the slab for two different conditions of wall emissivity, namely, $\varepsilon_0 = \varepsilon_L = 1$ and $\varepsilon_0 = \varepsilon_L = 0.7$. As shown in Fig. 6, the FVM results are in good agreement with the results obtained by Tan et al.[20] using the pseudo source adding method. The maximum relative error based on the data in Ref. 20 is less than 2%.

B. Apparent Directional Emissivity of a Two-Dimensional Rectangular Medium

As shown in Fig. 7, we consider a two-dimensional rectangular absorbing-emitting but nonscattering grey semitransparent medium with length $L = 0.1$ m and height $H = 0.1$ m. The boundaries are smooth and semitransparent surfaces. The medium is isothermal and surrounded by a vacuum. The absorption coefficient is uniform within the medium at $\kappa_a = 10\ \mathrm{m}^{-1}$, but the refractive index is a linear function of spatial position

$$n(x, y) = 1.1 + 0.6x/L + 0.2y/H \tag{26}$$

FVM is applied to solve for the apparent directional emissivity emerging from the plane $z =$ constant. The spatial domain is uniformly divided into $N_x \times N_y = 400 \times 400$ parts, and the angular domain into $N_\varphi = 360$ parts. Reflection and refraction at the boundary surfaces are treated according to Snell's and Fresnel's laws. The details can be seen in Ref. 21, and so will not be repeated here. Figure 8 shows the perpendicular component of apparent directional emisivity at the position $x = 0.025$ m and $y = 0.0$ m, and compared to the results obtained by Ben Abdallah et al.[4] using the curved ray-tracing method. As a whole, FVM results are in good agreement with the results obtained by the curved ray-tracing method. However, the sharp peaks of the emissivity profile are smoothed in the results

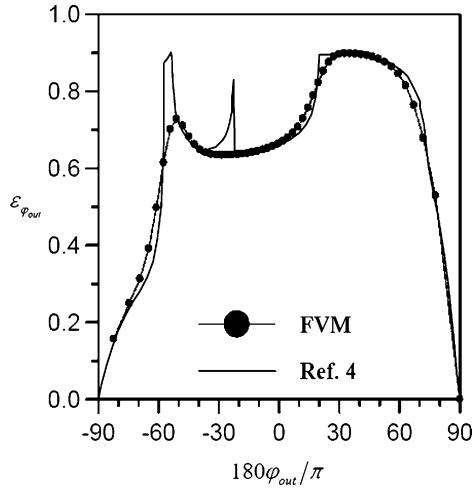

Fig. 8 Apparent directional emissivities emerging at the point $x = 0.025$ m and $y = 0.0$ m.

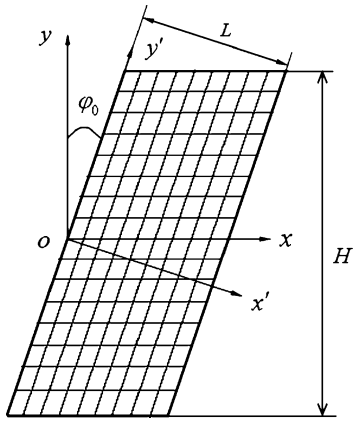

Fig. 9 Coordinate transfer and grid system.

obtained by FVM. Even so, the rms error, defined as follows, is less than 0.04,

$$E_{\mathrm{rms}} = \left[\frac{1}{\pi}\int_{-\pi/2}^{\pi/2} (\varepsilon_{\varphi_{\mathrm{out}},\mathrm{FVM}} - \varepsilon_{\varphi_{\mathrm{out}},\mathrm{ray-tracing}})^2\, \mathrm{d}\varphi_{\mathrm{out}}\right]^{\frac{1}{2}} \tag{27}$$

C. Radiative Equilibrium in a Two-Dimensional Medium

Recently, multidimensional radiative transfer within a graded index medium has been reported only by Ben Abdallah et al.[4] for the apparent emissivity of a two-dimensional rectangular medium with spatially variable refractive index. To further verify the finite volume formulation just presented for radiative transfer in the medium with variable spatial refractive index, we make a coordinate transformation in the one-dimensional problem solved in part A. As shown in Fig. 9, by transforming through an angle $\varphi_0 = \pi/6$ in the paper plane the coordinate system $x' - o - y'$ is transformed into $x - o - y$. Then, in the new coordinate system $x - o - y$ the variation of refractive is two dimensional as

$$n(x, y) = 1.2 + 0.6(x\cos\varphi_0 - y\sin\varphi_0)/L \tag{28}$$

FVM is applied to solve this two-dimensional radiative equilibrium problem in the new coordinate system $x - o - y$. The upper and lower boundaries are open boundaries. We are only interested in the temperature distribution for the domain near the site $y = 0$. As proposed by Liu and coworkers,[22,23] if the open boundaries are treated as black walls with local medium temperature, in order to get reasonable numerical results the open boundaries need to be set up far from the zone of interest, more than 2.0 optical thicknesses away. For the case of $\kappa_a = 10\ \mathrm{m}^{-1}$ and $\omega = 0$, in this paper the height is selected as $H = 1$ m so that the optical thickness based the half-height is $\tau_{H/2} = 5$.

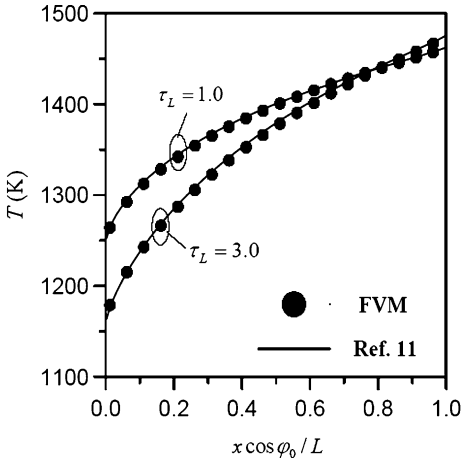

Fig. 10 Temperature distribution solved as two-dimensional problem for the case of $\varepsilon_0 = \varepsilon_L = 1$ and $\omega = 0$.

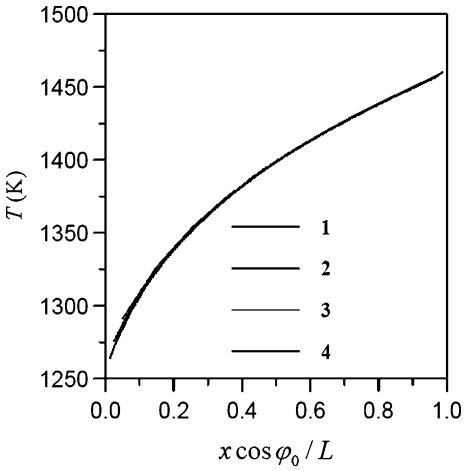

Fig. 11 Effects of number of control volumes and angular discretization in the case of $\tau_L = 1$, $\varepsilon_0 = \varepsilon_L = 1$, and $\omega = 0$: 1, $N_x \times N_y = 10 \times 20, N_\theta \times N_\varphi = 9 \times 18$; 2, $N_x \times N_y = 20 \times 40, N_\theta \times N_\varphi = 9 \times 18$; 3, $N_x \times N_y = 20 \times 40$, $N_\theta \times N_\varphi = 18 \times 36$; and 4, $N_x \times N_y = 40 \times 200$, $N_\theta \times N_\varphi = 18 \times 36$.

For this two-dimensional problem, the spatial computational domain is uniformly subdivided into $N_x \times N_y = 40 \times 200$ spatial control volumes, and the total solid angle is uniformly subdivided into $N_\theta \times N_\varphi = 18 \times 36$ control solid angles. The temperature distribution at $y = 0$ is shown in Fig. 10 for the case of $\tau_L = \kappa L = 1.0$, $\omega = 0$, and $\varepsilon_0 = \varepsilon_L = 1$, and is compared with the results found for the one-dimensional problem by using the pseudo source adding method. FVM results are in good agreement with the results obtained by using the pseudo source adding method. The maximum relative error based on the data in Ref. 11 is less than 1%.

The effects of number of control volumes and angular discretization are shown in Fig. 11 for the case of $\tau_L = 1$, $\varepsilon_0 = \varepsilon_L = 1$, and $\omega = 0$. The comparison is quite good, even with a mesh of only $N_x \times N_y = 10 \times 20$ and $N_\theta \times N_\varphi = 9 \times 18$. The convergence of the FVM is demonstrated in this figure.

IV. Conclusions

Because a ray goes along a curved path determined by the Fermat principle, curved ray tracing is very difficult and complex in a graded index medium. To avoid the complicated and time-consuming computation of curved ray trajectories, the original radiative-transfer equation is transformed so that the divergence theorem and finite volume integration can be easily used. Then, a finite volume formulation is developed to solve the radiative-transfer problem in a multidimensional absorbing-emitting-scattering semitransparent medium with variable spatial refractive index. Three test problems of radiative transfer are taken as examples to verify this finite volume formulation. The predicted temperature distributions and apparent directional emissivity are determined by the proposed method and compared with data in the references. The results show that the finite volume formulation presented in this paper has good accuracy in solving the radiative-transfer problem in a multidimensional absorbing-emitting-scattering semitransparent medium with variable spatial refractive index.

Acknowledgment

The support of this work by the National Nature Science Foundation of China (50336010) is gratefully acknowledged.

References

[1]Qiao, Y. T., *Graded Index Optics*, Science Press, Beijing, People's Republic of China, 1991, pp. 45–168.

[2]Siegel, R., and Spuckler, C. M., "Variable Refractive Index Effects on Radiation in Semitransparent Scattering Multilayered Regions," *Journal of Thermophysics and Heat Transfer*, Vol. 7, No. 4, 1993, pp. 624–630.

[3]Ben Abdallah, P., and Le Dez, V., "Temperature Field Inside an Absorbing-Emitting Semitransparent Slab at Radiative Equilibrium with Variable Spatial Refractive Index," *Journal of Quantitative Spectroscopy and Radiative Transfer*, Vol. 65, No. 4, 2000, pp. 595–608.

[4]Ben Abdallah, P., and Le Dez, V., "Thermal Emission of a Two-Dimensional Rectangular Cavity with Spatial Affine Refractive Index," *Journal of Quantitative Spectroscopy and Radiative Transfer*, Vol. 66, No. 6, 2000, pp. 555–569.

[5]Ben Abdallah, P., and Le Dez, V., "Thermal Emission of a Semitransparent Slab with Variable Spatial Refractive Index," *Journal of Quantitative Spectroscopy and Radiative Transfer*, Vol. 67, No. 3, 2000, pp. 185–198.

[6]Ben Abdallah, P., Charette, A., and Le Dez, V., "Influence of a Spatial Variation of the Thermo-Optical Constants on the Radiative Transfer Inside an Absorbing-Emitting Semitransparent Sphere," *Journal of Quantitative Spectroscopy and Radiative Transfer*, Vol. 70, No. 3, 2001, pp. 341–365.

[7]Liu, L. H., "Discrete Curved Ray-Tracing Method for Radiative Transfer in an Absorbing-Emitting Semitransparent Slab with Variable Spatial Refractive Index," *Journal of Quantitative Spectroscopy and Radiative Transfer*, Vol. 83, No. 2, 2004, pp. 223–228.

[8]Liu, L. H., Zhang, H. C., and Tan, H. P., "Monte Carlo Discrete Curved Ray-Tracing Method for Radiative Transfer in an Absorbing-Emitting Semitransparent Slab with Variable Spatial Refractive Index," *Journal of Quantitative Spectroscopy and Radiative Transfer*, Vol. 84, No. 3, 2004, pp. 357–362.

[9]Ben Abdallah, P., Fumeron, S., Le Dez, V., and Charette, A., "Integral Form of the Radiative Transfer Equation Inside Refractive Cylindrical Media," *Journal of Thermophysics and Heat Transfer*, Vol. 15, No. 2, 2001, pp. 184–189.

[10]Huang, Y., Xia, X. L., and Tan, H. P., "Radiative Intensity Solution and Thermal Emission Analysis of a Semitransparent Medium Layer with a Sinusoidal Refractive Index," *Journal of Quantitative Spectroscopy and Radiative Transfer*, Vol. 74, No. 2, 2002, pp. 217–233.

[11]Huang, Y., Xia, X. L., and Tan, H. P., "Temperature Field of Radiative Equilibrium in a Semitransparent Slab with a Linear Refractive Index and Gray Walls," *Journal of Quantitative Spectroscopy and Radiative Transfer*, Vol. 74, No. 2, 2002, pp. 249–261.

[12]Raithby, G. D., and Chui, E. H., "A Finite-Volume Method for Predicting a Radiant Heat Transfer Enclosures with Participating Media," *Journal of Heat Transfer*, Vol. 112, No. 2, 1990, pp. 415–423.

[13]Chui, E. H., Raithby, G. D., and Hughes, P. M. J., "Prediction of Radiative Transfer in Cylindrical Enclosures with the Finite Volume Method," *Journal of Thermophysics and Heat Transfer*, Vol. 6, No. 4, 1992, pp. 605–611.

[14]Chui, E. H., and Raithby, G. D., "Computation of Radiation Heat Transfer on a Nonorthogonal Mesh Using the Finite-Volume Method," *Numerical Heat Transfer, Part B*, Vol. 23, No. 3, 1993, pp. 269–288.

[15]Chai, J. C., Lee, H. S., and Patankar, S. V., "Finite Volume Method for Radiation Heat Transfer," *Journal of Thermophysics and Heat Transfer*, Vol. 8, No. 3, 1994, pp. 419–425.

[16]Chai, J. C., Parthasarathy, H. S., Lee, H. S., and Patankar, S. V., "Finite Volume Method Radiative Heat Transfer Procedure for Irregular Geometries," *Journal of Thermophysics and Heat Transfer*, Vol. 9, No. 3, 1995, pp. 410–415.

[17]Chai, J. C., Lee, H. S., and Patankar, S. V., "Treatment of Irregular Geometries Using a Cartesian Coordinates Finite-Volume Radiation Heat Transfer Procedure," *Numerical Heat Transfer, Part B*, Vol. 26, No. 3, 1994, pp. 225–235.

[18]Liu, J., Shang, H. M., and Chen, Y. S., "Development of Unstructured Radiation Model Applicable for Two-Dimensional Planar, Axisymmetric, and Three-Dimensioal Geometries," *Journal of Quantitative Spectroscopy and Radiative Transfer*, Vol. 66, No. 1, 2000, pp. 17–33.

[19]Liu, L. H., Tan, H. P., and Yu, Q. Z., "Temperature Distributions in an Absorbing-Emitting-Scattering Semitransparent Slab with Variable Spatial Refractive Index," *International Journal of Heat and Mass Transfer*, Vol. 46, No. 15, 2003, pp. 2917–2920.

[20]Tan, H. P., Huang, Y., and Xia, X. L., "Solution of Radiative Heat Transfer in a Semitransparent Slab with an Arbitrary Refractive Index Distribution and Diffuse Gray Boundaries," *International Journal of Heat and Mass Transfer*, Vol. 46, No. 11, 2003, pp. 2005–2014.

[21]Modest, M. F., *Radiative Heat Transfer*, 2nd ed., Academic Press, San Diego, 2003, p. 47.

[22]Liu, L. H., Ruan, L. M., and Tan, H. P., "On the Treatment of Open Boundary Condition for Radiative Transfer Equation," *International Journal of Heat and Mass Transfer*, Vol. 46, No. 1, 2003, pp. 181–183.

[23]Liu, L. H., "Domain Isolation Concept for Solution of Radiative Transfer in Large-Scale Semitransparent Media," *Journal of Quantitative Spectroscopy and Radiative Transfer*, Vol. 78, No. 3–4, 2003, pp. 373–379.